The crystal structure and luminescent properties of nitrogen-rich Ca-α-sialon:Eu with saturated calcium solubility fabricated by the alloy-nitridation method*

Yang Jian-Jun(杨建军), Chen Guo-Dong(陈国动),
Du Fei-Fei(杜飞飞), and Liu Quan-Lin(刘泉林)†

School of Materials Science & Engineering and State Key Laboratory for Advanced Metals and Materials, University of Science and Technology Beijing, Beijing 100083, *China*

(Received 24 November 2011; revised manuscript received 15 December 2011)

Nitrogen-rich Ca-α-sialon: Eu^{2+} phosphors with saturated calcium solubility are synthesized through a solid-state reaction (SSR) at 2173 K with stable alloy and nitride as the starting materials. The $Ca_{1.83-1.5x}Si_{8.34}Al_{3.66}O_xN_{16-x}$: xEu phosphors have intensive orange emissions, whose peaks are located at approximately 585–600 nm, and the emission wavelengths tend to shift toward the red region when the Eu concentrations increase from 0.5% to 18% (mole percentage). When the Eu concentration is equal to 9%, the phosphors suffer from concentration quenching. The low-temperature photoluminescence properties indicate that $Ca_{1.83-1.5x}Si_{8.34}Al_{3.66}O_xN_{16-x}$: xEu phosphors show excellent thermal quenching. The crystal structures of $Ca_{1.83-1.5x}Si_{8.34}Al_{3.66}O_xN_{16-x}$: xEu are also investigated, and are found to have nitrogen-rich compositions with saturated calcium cations at the interstitial sites of the α-sialons. In addition, the influencing factors of α-sialons with different compositions on the crystal lattice are discussed in detail.

Keywords: Ca-α-sialon, crystal structure, luminescence, alloy-nitridation

PACS: 78.55.Hx, 81.05.Je, 61.66.Fn **DOI:** 10.1088/1674-1056/21/7/077802

1. Introduction

Eu^{2+}-doped α-sialons have attracted considerable attention in recent years owing to their potential applications as down-conversion phosphors for white light-emitting diodes (LEDs). These kinds of materials combine high temperature and chemically stable α-sialons with the unique luminescence features of Eu^{2+} ions that exhibit parity-allowed, energy-efficient and broad 5d–4f absorption and emission.[1−4] The white LEDs will be a new generation of light sources that have the advantages of being energy-saving, with a long lifetime, compactness, and are environmentally friendly.[5] The white light can be generated by using an LED chip-phosphor system, in which the phosphor strongly absorbs ultraviolet (UV)–blue light (370–460 nm) from LED chips and efficiently re-emits in the red, green, or yellow parts of the visible spectrum. Typical commercially available white LEDs feature a combination of blue InGaN chips with $Y_3Al_5O_{12}$: Ce^{3+} (YAG:Ce)-based phosphors.[6] However, this type of white light has a high correlated colour temperature (CCT) and poor colour rendering index (CRI) because it lacks a red component, giving "cool"-white light. The demand for fabricating "warm"-white LEDs with a CCT of 2700–3200 K and a high CRI greater than 80 has driven LED phosphor development towards novel compositions and structure types. Currently, an important hot topic has focused on Eu^{2+}/Ce^{3+}-doped silicon-based oxynitride and nitride phosphors whose emission can cover the entire visible spectrum due to host lattice sensitivity of Eu^{2+}/Ce^{3+} 4f–5d transitions in spectral positions.[4] Generally, the 4f–5d transition energy can be lowered when Eu^{2+}/Ce^{3+} coordinates to a lower electronegative and higher formal charge nitrogen (N^{3-}) than oxygen (O^{2-}) due to the nephelauxetic effect (covalence) and the high ligand-field splitting of the 5d level.[7] This reasoning has led to extensive studies on Eu^{2+}/Ce^{3+}-doped (oxy)nitride phosphors, including representa-

*Project supported by the National Natural Science Foundation of China (Grant No. 90922027), the National High Technology Research and Development Program of China (Grant No. 2009AA03Z432), and the Doctoral Fund of Ministry of China (Grant No. 20100006110011).

†Corresponding author. E-mail: qlliu@ustb.edu.cn

© 2012 Chinese Physical Society and IOP Publishing Ltd

tive $M_2Si_5N_8:Eu^{2+}$ (M = Ca, Sr, Ba)[8−10] and $MAlSiN_3:Eu$ red phosphors, [11,12] $MSi_2O_2N_2:Eu^{2+}$ (M = Ca, Sr, Ba)[13,14] and $MYSi_4N_7:Eu$ (M = Sr, Ba) green-yellow phosphors,[15] and β/α-sialon : Eu green-yellow phosphors.[1,2,16]

Sialons constitute an important family of materials with unique structural features and various crystal chemistries. α-sialons are solid solutions of the M–Si–Al–O–N system, whose structure is derived from α-Si_3N_4, and can be represented as $M_xSi_{12-(m+n)}Al_{(m+n)}O_nN_{16-n}$, where m (Al–N) pairs and n (Al–O) pairs replace the $m+n$ (Si–N) pairs in each unit cell; $x = m/v$, with v being the valence of the M ion. M is a modifying cation, typically Li^+, Mg^{2+}, Ca^{2+}, Y^{3+} or rare-earth (RE) with $Z > 60$.[17] In the α-sialon structure there are two interstitial sites per unit cell which can accommodate M cations. Thus, the M content (x) is less than or equal to 2, and the values of m and x are taken to meet the electroneutrality requirement, i.e., $x = m/v$. Because of their excellent mechanical properties and high-temperature stability, α-sialon ceramics have been developed for structural engineering applications. Since the pioneering work of Krevel *et al.*[1] and Xie *et al.*[2] in 2002, RE-doped α-sialon phosphors have received increasing attention. In particular, Ca-α-sialon : Eu, which exhibits yellow emission (about 570–600 nm) and a strong absorption in the UV to the blue spectral range (about 300–470 nm), has been proved to be a good down-conversion phosphor for white LEDs combined with blue InGaN LED chips.[3]

According to the previous work, when the m value is in a range of $3.0 \leq m \leq 4.0$, the Ca-α-sialon phosphors have excellent photoluminescence properties.[3,18] The emission intensity of Ca-α-sialon monotonously increases with the m value and reaches a maximum when the $m/2$ value approaches a saturated calcium solubility of approximately 1.83 (m = 3.66). These results may be induced by either the energy transfer (due to the concentration of modifying cations) or the crystallinity of the host (due to the presence of impurity phases). The emission intensities decrease with an increase in the n values or the oxygen content. Because there are only two interstitial sites per unit cell for these modifying cations, the upper limiting compositions for α-sialons with a v-valence metal ion are expected to be $M_2Si_{12-2v}A1_{2v}N_{16}$, e.g., $Ca_2Si_8A1_4N_{16}$. These limits have not been achieved possibly due to the presence of oxygen in the silicon nitride particles.[17] The highest solubility was reported to be 1.83 Ca^{2+} per cell in Ca-α-sialon with a composition of $Ca_{1.83}Si_{8.34}Al_{3.66}N_{16}$. The upper limit of the solubility in α-sialon generally decreases as the size of the modifying cation becomes larger.[17] Generally, the Eu^{2+} ion alone cannot incorporate into and stabilize the α-sialon structure due to its large size, but it does if co-doped with Ca^{2+} or Y^{3+}.[1] However, recently Hirosaki *et al.*[16] reported on the synthesis and luminescent properties of Eu single-doped α-sialon prepared by a solid-state reaction (SSR). As to the Eu^{2+}-doped Ca-α-sialon, the sample with the upper limit m value ($m = 3.66$) has more intensive emission than that with a smaller m value.[3,18] The investigation by Shioi *et al.*[19] also suggested that the concentration of trivalent Eu^{3+}, which could be a luminescent killer centre, monotonically increases with the increase in oxygen content (n). From the experimentally phenomenological viewpoint, the high m value (calcium solubility) and low n value may make beneficial contributions to the emission wavelength red shift and intensity enhancement of Ca-α-sialon : Eu. The wavelength red shift of nitrogen-rich Ca-α-sialon: Eu will meet the high CRI and low CCT requirements of LED lamps and the high spectral luminous efficiencies (SLE) to human eyes.

The Eu^{2+}-doped oxygen-rich Ca-α-sialon phosphors ($Ca_xSi_{12-(m+n)}Al_{(m+n)}O_nN_{16-n}$: xEu^{2+} with larger n values), have been extensively investigated due to easy control of their compositions. In contrast, studies of Eu^{2+}-doped nitrogen-rich Ca-α-sialon phosphors ($Ca_{m/2}Si_{12-m}Al_mN_{16}:Eu^{2+}$ with zero or very small values of n) are very limited due to the fact that it is difficult to control the compositions because of the oxygen and moisture sensitivity of the alkaline earth metals or nitride starting materials. Recently, Piao *et al.*[20] reported on the synthesis and luminescent properties of low oxygen ($\leq$0.7wt.%) contained Ca-α-sialon : Eu^{2+} from cyanamide reduction, and Park *et al.*[21] prepared Eu^{2+}-doped nitrogen-rich Ca-α-sialon through the gas reduction nitridation (GRN) method with nitride as the starting material and Eu_2O_3 as the dopant.

To the best of our knowledge, up until now, there has been no report on the systematic investigation of nitrogen-rich Ca-α-sialon : Eu^{2+} with saturated calcium cations in α-sialon, i.e., nitrogen-rich Ca-α-sialon : Eu^{2+} with the upper limit m value ($m = 3.66$, e.g., for $Ca_{1.83}Si_{8.34}Al_{3.66}O_nN_{16-n}:Eu^{2+}$, $n \leq 0.329$), which may have excellent photoluminescence properties. The nitrogen-rich and high m value composi-

tion may make good crystallinity, giving strong emission intensities. The nephelauxetic effect and anion polarizability of the nitrogen-rich structure may give long wavelength emissions, and the nitrogen-rich perfect rigid framework may provide a crystal chemistry basis for good concentration quenching and thermal quenching properties. In the past few years, some methods have been tried to synthesize the Eu^{2+}-doped sialon phosphors, such as SSR at high temperature and high pressure,[2] carbothermal reduction nitridation (CRN),[22,23] and gas reduction nitridation (GRN) methods,[18,24] gas-pressured sintering (GPS),[25] and spark plasma sintering (SPS).[26] The SSR method has advantages in improving the luminescent efficiencies of phosphors and large-scale production. In this work, we investigate the crystal structure and photoluminescence properties of the nitrogen-rich sialon phosphors with $Ca_{1.83}Si_{8.34}Al_{3.66}N_{16}$ as the host, which are synthesized through SSR with stable CaAl alloys and nitrides as the starting materials.

2. Experiments

The starting materials included CaAl alloy, AlN and Si_3N_4 powders, and the purities of all raw materials were above 99.5% in quality proportion. The starting materials were stoichiometrically weighted according to the compositions of $Ca_{1.83-1.5x}Si_{8.34}Al_{3.66}O_xN_{16-x} : xEu^{2+}$ (the value of x is the mole percentage of doped Eu, and the mole percentages were 0.5%, 2%, 4%, 6%, 9%, 12%, 15%, and 18% respectively). Then the materials were mixed and ground in an agate mortar into fine powder with n-hexane as the dispersant to avoid oxidation. The powder was pressed into pellets and sequentially placed into a graphite furnace. The furnace chamber was pressurized to 0.3 MPa starting with high-purity nitrogen atmosphere ($> 99.99\%$) after being vacuumed to 10^{-3} Pa below. The samples were sintered at 2173 K for 4 h. After the furnace was cooled to room temperature, the as-prepared samples were crushed and ground into fine powder for further investigations on the crystal structure and photoluminescence properties.

The emission and excitation spectra at room temperature were recorded on an Edinburgh FL920 fluorescence spectrophotometer with a Hamamatsu S900-R (red sensitive version) photomultiplier tube (PMT). The spectrum resolution was 1.0 nm. The monochrometer slits for both excitation and emission were kept at 0.3 nm, and the dwell period at each wavelength (dwell time) was 0.30 s. The wavelength scan speed was 200 nm/min, and the spectral scan region covered at least 450–700 nm. The same instrumental settings were applied in all measurements for comparison. The emission and excitation spectra at low temperature were also tested on the FL920 fluorescent spectrometer without PMT. The spectral scan maximum extended to 800 nm, and the scan step was 0.1 nm. Using a closed loop liquid helium refrigeration system, we acquired the spectra at low temperature through cooling the samples to 10–350 K.

The X-ray diffraction (XRD) data for structure analysis were collected on a Philips X'Pert PW-3040 diffract meter (45 kV, 40 mA) with Cu K_α radiation ($\lambda = 0.15406$ nm). A continuous scan mode was employed with a step width of 0.02° in 2θ. The scan angle was 10°–70°, and the XRD data were analysed on the Rietveld refinement program FullProf.2k (version 2.40)

3. Results and discussion

3.1. XRD patterns and crystal structure analysis

Generally, phosphor consists of a host and activators or a luminescence centre. For our samples, the $Ca_{1.83}Si_{8.34}Al_{3.66}N_{16}$ host is nitrogen-rich α-sialon with calcium solubility saturation and the luminescence centres are Eu^{2+} divalent ions, which occupy the crystallographic sites of modifying cations (Ca sites). In order to investigate the effect of Eu concentration on the crystal structure and luminescence property, the concentrations of Eu were kept at a very low level, i.e., 0.009–0.329 (0.5%–18.0% mole percentage). Thus, the crystal structures of Ca-α-sialon with different values of Eu concentration are not expected to be modified by Eu dopant.

Phase analysis was first conducted on the XRD data of Ca-α-sialon samples in a range of 15°–68°, as shown in Fig. 1. The XRD patterns match well with those of the previously reported Ca-α-sialon[1,2] (JCPDS No. 48-1586), and all the compositions of the samples are pure α-sialon phases. The crystal structures of the samples belong to a trigonal system, and the space group is $P31c$ (159). Further analysis on the lattice parameters was made using the Rietveld profile fitting technique with the FULLProf

program.[27] The Rietveld refinement reliability factors are $R_{wp} \leq 13.2\%$ and $R_{exp} \leq 10.2\%$. The relationship between the lattice parameters and the Eu concentration is obtained through Rietveld refinement results and the lattice parameters are listed in Table 1.

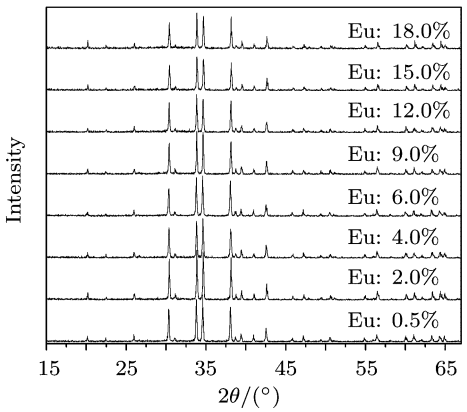


Fig. 1. XRD patterns of $Ca_{1.83-1.5x}Si_{8.34}Al_{3.66}O_xN_{16-x}$: xEu samples.

Table 1. The crystal lattice parameters of the investigated samples.

x/%	a/Å	c/Å	V/Å^3
0.5	7.8992	5.7365	309.986
2	7.9020	5.7371	310.238
4	7.9039	5.7380	310.439
6	7.9116	5.7420	311.259
9	7.9044	5.7388	310.525
12	7.9005	5.7360	310.063
15	7.8931	5.7319	309.266
18	7.8877	5.7304	308.758

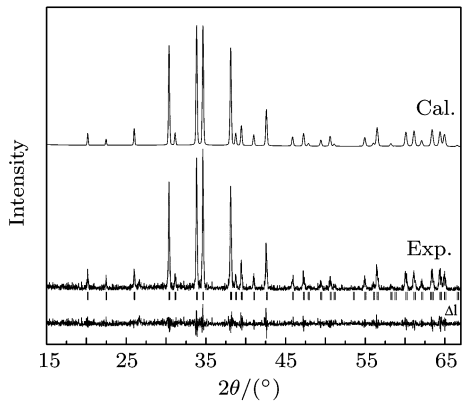


Fig. 2. XRD Rietveld refinement of a typical $Ca_{1.83-1.5x}Si_{8.34}Al_{3.66}O_xN_{16-x}$: xEu sample.

The errors of the lattice parameters from Rietveld refinement are less than 0.0001 Å (1 Å = 0.1 nm). The Eu^{2+}-doped Ca-α-sialon with calcium solubility saturation has a composition of $Ca_{1.83-1.5x}Si_{8.34}Al_{3.66}O_xN_{16-x}$: xEu^{2+} due to the presence of oxygen from the Eu_2O_3 dopant. Figure 2 shows the Rietveld refinement results from the XRD patterns of a typical Ca-α-sialon sample with the composition $Ca_{1.83-1.5x}Si_{8.34}Al_{3.66}O_xN_{16-x}$: xEu^{2+} ($x = 0.329$), including the Bragg reflection positions, the experimental and calculated intensities, as well as the difference intensities between the experimental and calculated data.

Based on the data in Table 1, the relationship between the crystal lattice parameters (a, c) and the Eu concentration is shown in Fig. 3. The lattice parameters (a, c) increase with increasing Eu concentration, and tend to reach their maximal values at a mole percentage of approximately 6%. The crystal structure of α-sialons typically consists of [(Si,Al)(N,O)$_4$] tetrahedrons, in which the m Al–N bond (0.187 nm) replaces the m Si–N bond (0.174 nm) and the n Al–O bond (0.175 nm) replaces the n Si–N bond (0.174 nm). The tetrahedron units are stacked together by sharing their corners to form a condensed, rigid framework, with Ca^{2+} and Eu^{2+} cations in the interstitial holes of the [Si,Al]–[O,N] network, resulting in excellent thermal and chemical stability. The Al^{3+} and Si^{4+} ion sites are both four-coordinated, and the Si^{4+} and Al^{3+} ions occupy the equivalent sites with disordered distribution. In the range of Eu concentrations below 6%, the lattice parameters (a, c) increase monotonically with increasing Eu concentration, because the radius of Eu^{2+} (1.20 Å) is larger than that of Ca^{2+} (1.06 Å), and the solubility of Eu^{2+} incorporated into the Ca-α-sialon lattice monotonically increases in this range. Moreover, in this Eu concentration range, the influence of trace amount O^{2-} anion on the lattice parameter is very small because a part of the O^{2-} anions are reduced and the rest incorporate into the Ca-α-sialon lattice by substituting N^{3-} anions. In the range of Eu concentrations beyond 6% and below 18%, the lattice parameters (a, c) decrease linearly with increasing Eu concentration, because the interstitial sites are mostly occupied by Ca^{2+} and Eu^{2+} ions, and the solubility of Eu^{2+} in Ca-α-sialon is saturated. The linear decrease in the lattice parameters with increasing Eu concentration indicates that more O^{2-} anions are incorporated into the lattice. The radius of the O^{2-} anion is smaller than that of the N^{3-} anion, and the lattice volume (V) decreases linearly with O^{2-} incorporating increasingly into Ca-α-sialon as the Eu_2O_3 dopant. The subtle combination of the above two influencing sides can give rise to the complex dependence of lattice parameters on Eu concentration (or the value of

x) in the $Ca_{1.83-1.5x}Si_{8.34}Al_{3.66}O_xN_{16-x}$: xEu composition, as shown in Fig. 3. de Graaf *et al.* support that the presence of N^{3-} as the anionic net former in crystal or glass leads to the reduction in potential according to $6Eu^{3+}+2N^{3-} \rightarrow 6Eu^{2+}+2N_2$.[28] Therefore, only the divalent Eu^{2+} emission is observed in phosphors even though the Eu_2O_3 oxide is used for the conventional SSR from the nitride starting materials (Ca_3N_2, AlN, Si_3N_4). During the synthesis of our samples, due to trace amounts of Eu_2O_3 dopant, the graphite (C) heater may supply a reducing environment, giving the reducing potential through carbothermal reduction-nitridation (CRN) SSR under high-purity nitrogen atmosphere according to $2Eu^{3+}+O^{2-}+C \rightarrow 2Eu^{2+}+CO$.

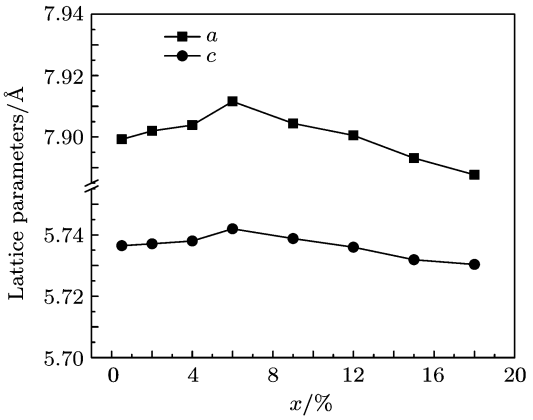


Fig. 3. The relationship between the crystal lattice parameters and the Eu concentration in Ca-α-sialon.

Table 2 demonstrates several isostructural α-sialons that have the same space group ($P31c$, 159). From Table 2, the non-oxygen composition of $Ca_{1.83}Si_{8.34}Al_{3.66}N_{16}$ in note ① has larger crystal lattice parameters than our $Ca_{1.83-1.5x}Si_{8.34}Al_{3.66}O_xN_{16-x}$: xEu samples mainly because of the crystal lattice contraction resulting from O^{2-} incorporation into the lattice. The $Ca_{1.71}Si_{8.57}Al_{3.43}N_{16}$: Eu sample has a smaller lattice than the $Ca_{1.83-1.5x}Si_{8.34}Al_{3.66}O_xN_{16-x}$: xEu samples because of the different Al/Si ratios (m). Both of them have much larger crystal lattice parameters than those of notes ② and ③. This is ascribed mainly to the much higher Al/Si ratios (≥ 0.4) of the former two (Al/Si = 0.3 or 0.2 for the latter). Because of their much larger radius, we suppose that the lattice variation is partially attributed to the ion concentrations of Ca^{2+} and Eu^{2+}, which are incorporated into the interstitial sites of the [Si,Al]–[O,N] network, although some have supported the argument that the size and solubility of the modifying cations have little influence on the lattice expansion of α-sialon. This possibly stands on the assumption that the interstitial holes are large enough to accommodate those cations.[17] For our samples, because both a lower O^{2-} content and more Ca^{2+} ions are substituted by more Eu^{2+} at the interstitial sites, the crystal lattice parameters increase with the Eu concentration rising within 6%, although they have the same Al/Si ratios (Fig. 3). The α-$Si_{12}N_{16}$ in note ④ has the smallest crystal lattice volume because of its condensed, rigid framework formed by small pure [SiN_4] tetrahedrons. In conclusion, the influencing factors on the crystal lattice parameters of α-sialons with different compositions are mainly as follows.

1) For the Al/Si ratio (m), the larger the value of m, the larger the crystal lattice parameters are.

2) For the O/N ratio (n), the larger the value of n, the smaller the crystal lattice parameters are.

3) For the modifying cations incorporating into the interstitial sites, the higher the solubility and the larger the modifying cations, the larger the crystal lattice parameters are.

Table 2. The lattice parameters of different compositions of α-sialon and α-$Si_{12}N_{16}$.

α-sialon	a/Å	c/Å	V/Å^3	notes
$Ca_{1.83}Si_{8.34}Al_{3.66}N_{16}$	7.955	5.769	316.163	① Ref. JCPDS. 48-1586 (1996)
$Ca_{1.83-1.5x}Si_{8.34}Al_{3.66}O_xN_{16-x}$: xEu	7.900	5.736	310.067	our work
$Ca_{1.71}Si_{8.57}Al_{3.43}N_{16}$: Eu	7.894	5.733	309.422	our work
$Ca_{0.8}Si_{9.2}Al_{2.8}O_{1.2}N_{14.8}$	7.852	5.709	304.825	② Ref. JCPDS. 33-0261 (1978)
$Ca_{0.68}Si_{9.96}Al_{2.04}O_{0.68}N_{15.32}$	7.838	5.703	303.420	③ Ref. JCPDS. 42-0252 (1984)
α-$Si_{12}N_{16}$	7.758	5.623	293.088	④ Ref. JCPDS. 09-0250 (1958)

3.2. Photoluminescence properties

The excitation spectra of the $Ca_{1.83-1.5x}Si_{8.34}Al_{3.66}O_xN_{16-x}$: xEu samples are shown in Fig. 4. The excitation spectra include two broad bands. One band has a peak located at approximately 305 nm, in the ultraviolet range, and the other is a wide band located in a blue light range of 350–500 nm, matching the

blue InCaN chip. In general, the Eu^{2+} ion presents two broadband absorption peaks. The first one is assigned to absorption of the host lattice (α-sialon), and the second corresponds to the transition between the $4f^7$ ground state and the $4f^65d^1$ excitation state of Eu^{2+}.[3] The Eu-doped Ca-α-sialon phosphor matches with not only ultraviolet but also blue light excitation.

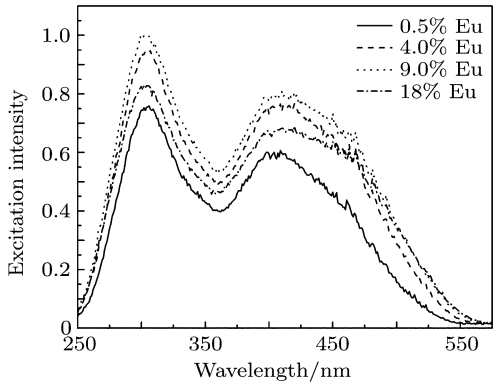


Fig. 4. The excitation spectra of Eu^{2+}-doped Ca-α-sialon samples with different concentrations.

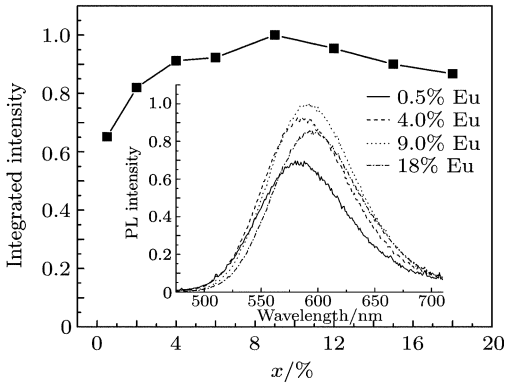


Fig. 5. The variation in the integrated intensity of the emission band with Eu^{2+} concentration (by 420 nm excitation). The insert is the photoluminescence (PL) intensity versus wavelength.

Figure 5 shows the emission spectra of the $Ca_{1.83-1.5x}Si_{8.34}Al_{3.66}O_xN_{16-x}$: xEu samples (see inset), and the relationship of the integrated intensities of the emission bands with the Eu^{2+} concentrations (by 450 nm excitation). The emission bands by 450 nm excitation are broad bands in a range of 500–700 nm, and the emission peaks are located in a range of approximately 585–600 nm. This is attributed to the dipole transition between the $4f^7$ state and $4f^65d^1$ state of the Eu^{2+} ions. The activators are divalent Eu^{2+} ions doped in the Ca-α-sialon crystal lattice. The integrated intensity of the sample first increases, then slowly decreases, and reaches a maximal intensity at an Eu^{2+} concentration of 9%. This indicates that the phosphors suffer from concentration quenching when the Eu concentration is equal to or above 9%.

The relationship between emission wavelength and Eu concentration is illustrated in Fig. 6. The emission peak position shifts toward long wavelengths with rising Eu concentration. The emission wavelength monotonically increases approximately 15 nm from 585 to 600 nm as the Eu concentration rises from 0.5% to 18%, which yields the body colour of the phosphors, varying from yellow to orange. The probability of energy transfer between two activator ions is inversely proportional to the n-th power of R' ($n = 6$, 8, or 10), where R' is the distance between activator ions. As the Eu concentration increases, the distance between Eu^{2+} ions becomes smaller. The change in crystal field may result in the splitting of the 5d level of Eu^{2+}. Therefore, the probability of the energy transfer from Eu^{2+} ions at higher 5d levels to those at lower 5d levels increases with the increase in Eu concentration. This makes it possible for the higher Eu^{2+} concentration to reduce the emission energy because the transition energy from the lower 5d excited state to the 4f ground state is smaller than that from the higher 5d to 4f ground state. Hence, this mechanism shifts the emission to a longer wavelength.

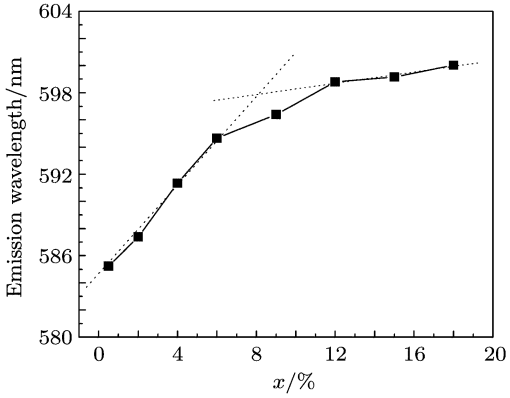


Fig. 6. The peak position of the emission band with respect to Eu^{2+} concentration (by 420 nm excitation).

According to Blasse, if the activators are introduced solely on Ca^{2+} ion sites, which are replaced by Eu^{2+} activators, the average space occupied per activator is expressed as the following equation:

$$\frac{V}{Nx_c} = \frac{4\pi}{3}R_a^3, \tag{1}$$

where, x_c is the critical concentration, N is the number of Ca^{2+} ions in the unit cell, and V is the volume

of the unit cell. The critical transfer distance is approximately equal to twice the radius of a sphere with this volume

$$R_{\rm c} = 2R_{\rm a} = 2 \times \left(\frac{3V}{4\pi N x_{\rm c}}\right)^{1/3}. \quad (2)$$

In our work, $R_{\rm c}$ is calculated to be 1.53 nm (V = 0.31053 nm^3, $N = 1.83$). The energy transfer between two luminescent centres may occur due to multipolar interaction, radiation reabsorption, or exchange. The exchange interaction, whose critical distance is approximately 0.5 nm, hardly plays any role in the energy transfer between two Eu^{2+} ions. Thus, based on the calculated critical distance and the spectral overlap of the excitation and emission bands, it is confirmed that multipolar interaction and radiation reabsorption are dominantly responsible for the energy transfer between two Eu^{2+} ions.

There are two factors influencing the emission wavelength of the Eu^{2+} ions. One is the Eu concentration incorporated into the α-sialon lattice. The wavelength monotonically increases with the increase in Eu concentration within 9%, in which there is a large ramp slope of emission wavelength with respect to Eu concentration. This is attributed to the fact that the enhanced multipolar interaction and radiation reabsorption make the emission wavelength shift toward the red region due to the smaller distance between activator ions with increasing Eu concentration. The other factor is related to the nephelauxetic effect (covalence) around the activator ions. With more N^{3-} ions substituted by high-electronegativity O^{2-} ions, the weak covalence of oxygen-contained $[(Si,Al)(ON)_4]$ tetrahedron structures elevates the centroid of the 5d energy level. This makes the emission wavelength shift toward the blue region. The XRD results show that the lattice parameters decrease monotonically with increasing Eu concentration over 9% (Fig. 3). This lattice contraction results from more oxygen being incorporated into the α-sialon lattice due to the Eu_2O_3 dopant. The wavelength increases on a small ramp slope of emission wavelengths with respect to an Eu concentration beyond 9%. The subtle combination of the above two factors can give rise to the complex dependence of the emission wavelength on Eu concentration (x) in $Ca_{1.83-1.5x}Si_{8.34}Al_{3.66}O_xN_{16-x}$: xEu compositions, as shown in Fig. 6. The Eu-doped Ca-α-sialon phosphors each have an intense orange emission when they are excited not only by ultraviolet but also by blue light. Because these phosphors contain a certain quantity of red colour component, white light with a higher CRI and lower CCT can be combined with the blue light of an InGaN LED chip.

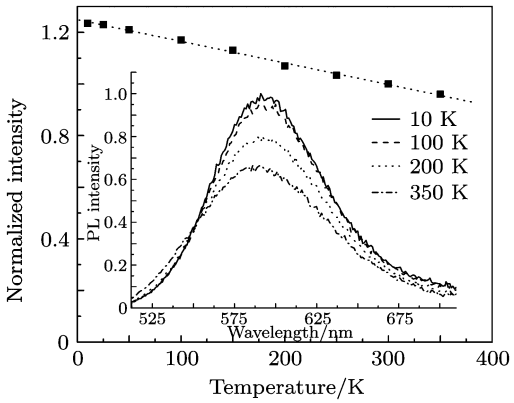


Fig. 7. The dependences of normalized emission intensity on temperature (by 450 nm excitation). The insert is PL intensity versus wavelength.

The PL spectra of the 9% Eu-doped $Ca_{1.83-1.5x}Si_{8.34}Al_{3.66}O_xN_{16-x}$: xEu samples in a temperature range of 10–350 K have been measured (see the insert in Fig. 7). The emission intensities monotonically decrease with temperature. As shown in the inset, when temperature increases from 10 to 350 K, the profiles of the emission peaks show no appreciable change. The emission wavelengths almost show no shift. This suggests that the Stokes shifts of the phosphors are stable against temperature, which may be attributed to the perfect rigid framework of Ca-α-sialon. Hence, the chromaticity coordinates of the phosphors are stable with respect to varying temperature, which indicates that the $Ca_{1.83-1.5x}Si_{8.34}Al_{3.66}O_xN_{16-x}$: xEu phosphors have excellent temperature stability and can work in a wide temperature range. When the temperature increases from 10 to 350 K, the emission intensities decrease by 23% of the initial value. Comparing one of our Ca-α-sialon phosphors ($Ca_{1.83-1.5x}Si_{8.34}Al_{3.66}O_xN_{16-x}$: xEu, x = 9 %) with the low oxygen contained $Ca_{0.90}Al_2Si_{10}N_{16}$:0.10$Eu^{2+}$ reported by Piao *et al.*, whose emission intensity decreases by 22% of the initial value, when the temperature increases from 4 to 280 K,[20] we suppose that our $Ca_{1.83-1.5x}Si_{8.34}Al_{3.66}O_xN_{16-x}$: xEu samples present better thermal quenching because of their more perfectly rigid nitrogen-rich structures than the structure of the oxygen contained sialon. As to the nitrogen-rich $Ca_{1.83-1.5x}Si_{8.34}Al_{3.66}O_xN_{16-x}$: xEu with saturated calcium solubility, the quenching temperature,[29] de-

fined as the temperature at which the emission intensity drops 50% of that measured at 300 K, can be estimated to be 893 K, which is much higher than that of the other oxonitridosilicates and oxide phosphors.[29−31]

4. Conclusions

We synthesized nitrogen-rich Ca-α-sialon : Eu^{2+} phosphors with saturated calcium solubility through SSR, with stable alloys and nitrides used as the starting materials. The $Ca_{1.83-1.5x}Si_{8.34}Al_{3.66}O_xN_{16-x}$: xEu phosphors each have an intensive orange emission, and the emission wavelengths tend to shift toward the red region with increasing Eu concentrations, which can meet the requirement of white light with higher CRI and lower CCT. The excellent thermal quenching properties make $Ca_{1.83-1.5x}Si_{8.34}Al_{3.66}O_xN_{16-x}$: xEu phosphors promising in white LED illumination. We investigated the crystal structures of $Ca_{1.83-1.5x}Si_{8.34}Al_{3.66}O_xN_{16-x}$: xEu, which have nitrogen-rich compositions with saturated calcium cations at interstitial sites of α-sialon, and discussed in detail the influencing factors on the crystal lattice of α-sialon with different compositions.

References

[1] van Krevel J W H, van Rutten J W T, Mandal H, Hintzen H T and Metselaar R 2002 *J. Solid State Chem.* **165** 19

[2] Xie R J, Mitomo M, Uheda K, Xu F F and Akimune Y 2002 *J. Am. Ceram. Soc.* **85** 1229

[3] Xie R J, Hirosaki N, Mitomo M, Yamamoto Y, Suehiro T and Sakuma K 2004 *J. Phys. Chem.* B **108** 12027

[4] Xie R J and Hirosaki N 2007 *Sci. Technol. Adv. Mater.* **8** 588

[5] Malakoff D 2002 *Science* **296** 1782

[6] Schubert E F and Kim J K 2005 *Science* **308** 1274

[7] Derenbos P 2002 *J. Alloys Compd.* **341** 156

[8] Höppe H A, Lutz H, Morys P, Schnick W and Seilmeier A 2000 *J. Phys. Chem. Solids* **61** 2001

[9] Li Y Q, de With G and Hintzen H T 2006 *J. Lumin.* **116** 107

[10] Wei X D, Cai L Y, Lu F C, Chen X L, Chen X Y and Liu Q L 2009 *Chin. Phys.* B **18** 3555

[11] Uheda K, Hirosaki N, Yamamoto Y, Naito A, Nakajima T and Yamamoto H 2006 *Electrochem. Solid-State Lett.* **9** H22

[12] Piao X Q, Ken-ichi M and Takashi H 2007 *Chem. Mater.* **19** 4592

[13] Florian S, Oliver O, Henning A H, Manfred H M, Rainer P, Bernd D M, Peter S, Viola D, Arndt S and Wolfgang S 2006 *Chem. Eur. J.* **12** 6984

[14] Volker B, Thomas J, Andries M, Cees R and Peter J S 2006 *J. Lumin.* **121** 441

[15] Li Y Q, Fang C M, de With G and Hintzen H T 2004 *J. Solid State Chem.* **177** 4687

[16] Hirosaki N, Xie R J, Kimoto K, Sekiguchi T, Yamamoto Y, Suehiro T and Mitomo M 2005 *Appl. Phys. Lett.* **86** 211905

[17] Cao G Z and Metselaar R 1991 *Chem. Mater.* **3** 242

[18] Li H L, Xie R J, Hirosaki N, Suehiro T and Yajima Y 2008 *J. Electrochem. Soc.* **155** J175

[19] Shioi K, Hirosaki N, Xie R J, Takeda T and Li Y Q 2010 *J. Alloys Compd.* **504** 579

[20] Piao X Q, Ken-ichi M, Takashi H and Hiromasa H 2008 *J. Rare Earths* **26** 198

[21] Park W J, Song Y H, Moon J W, Kang S M and Yoon D H 2010 *Solid State Sci.* **12** 1853

[22] Qiu J Y, Tatami J, Zhang C, Komeya K, Meguro T and Cheng Y B 2002 *J. Eur. Ceram. Soc.* **22** 2989

[23] Van Rutten J W T, Terpstra R A, Van der Heijde J C T, Hintzen H T and Metselaar R 1995 *J. Eur. Ceram. Soc.* **15** 599

[24] Li H L, Hirosaki N, Xie R J, Suehiro T and Mitomo M 2007 *Sci. Technol. Adv. Mater.* **8** 601

[25] Ryu J H, Park Y G, Won H S, Kim S H, Suzuki H, Lee J M, Yoon C, Nazarov M, Noh D Y and Tsukerblat B 2008 *J. Electrochem. Soc.* **155** J99

[26] Choi S W and Hong S H 2010 *J. Electrochem. Soc.* **157** J297

[27] Rietveld H M 1969 *J. Appl. Crystallogr.* **2** 65

[28] de Graaf D, Hintzen H T, Hampshire S and de With G 2003 *J. Eur. Ceram. Soc.* **23** 1093

[29] Lu F C, Song X P and Liu Q L 2011 *J. Alloys Compd.* **509** 2099

[30] Zhou T L, Song Z, Song X P, Bian L and Liu Q L 2010 *Chin. Phys.* B **19** 127808

[31] Lu F C, Chen X Y, Wang M W and Liu Q L 2011 *J. Lumin.* **131** 336